DEFLECTION ANALYSIS OF AERO GAS TURBINE STRUCTURE DURING PROTOTYPE DEVELOPMENT

M.Chandrasekaran*, and K.Ramachandra*

Gas Turbine Research Establishment,
Bangalore 560 093, INDIA.

ABSTRACT

This paper presents a refined finite element procedure to obtain the cold dimensions of aero engine structural assembly from the dimensions of larger hot gas flow path and also establish the operating clearances between rotor blades and casings. The effects of stiffness distribution on the circularity of casings-frames assembly and its weight optimization are also discussed.

* Scientist

INTRODUCTION

Aero engines are designed for their typical operating conditions, when the engine is hot. The engine's dimensions are different when it is cold, and these differences must be allowed for in fabricating the parts. Therefore, there is a need for preparing the cold lay-up for the engine. If the engine structure is poorly designed without the displacement analysis of the complete engine assembly, a significant engine performance loss can result from blade rubs caused by structural deflections. Several investigators[1,2,3] have reported studies on dynamic characteristics of aero engine structures. However, published literature on deflection analysis is practically non-existent.

A typical twin spool aero gas turbine engine (Fig.1 and Fig.2) consists of a fan, compressor, combustor, high pressure turbine, low pressure turbine and an exhaust nozzle. The rotating components e.g. the blades, disks, shafts and other accessories are assembled with bearing housings through a combination of ball and roller bearings located along the engine axis. The entire rotating assembly is housed in thin cylindrical shell structures which in turn are attached to the engine frames. The thrust generated by the engine is transmitted to the aircraft through mounting blocks in the frames.

The engine structural assembly consisting of frames, casings and mounts enable an engine to maintain rigid shape within specified tolerances, while withstanding enormous internal pressures and temperatures. In addition to providing the needed strength, rigidity and heat resistance, engine structures need to be as light as possible to meet low weight-to-thrust ratio. The increased engine performance is achieved by minimizing the clearances between the rotor and the stator casings. It is therefore important to be able to predict accurately the axial and radial displacements of an engine structural assembly well before the prototype is developed. This difficulty is further compounded by the differences that exist in the hot and cold lay-ups as explained earlier. This requires complex and detailed analysis in addition to powerful computer capabilities for the finite element modelling of the full scale engine structure.

In the present paper, procedure to obtain the cold dimensions of the engine structural assembly from the larger hot dimensions, is presented. The problems encountered while improving the circularity of the casings especially fan, compressor and turbine casings, are discussed. Strain energy distribution in the engine structural assembly was employed to optimize the engine weight.

FINITE ELEMENT MODEL

In order to optimize the time and effort required for the model generation, only 180 degree segment on one side of the vertical plane passing through the engine axis was considered [2]. It was decided to model the engine into its major substructures such as fan case, compressor case, combustor case, turbine case, engine frames, etc.,(Fig. 2). This was carried out for the superelement analysis of MSC/NASTRAN. The 180 degree half engine structural model with suitable boundary conditions along the reflective symmetric plane is therefore sufficient to represent the entire engine structure. The three dimensional model was constructed using shell, brick and beam elements.

Four noded CQUAD4 and three noded CTRIA3 shell elements were used for modelling the casings and frames (Fig. 3). The front mount block was modeled with eight noded HEXA and six noded PENTA elements. Two noded bar elements were used to stiffen the shell in ISO grid fan duct. Tie rods of aft frame were modeled with two noded ROD elements.

In order to reduce the error involved in the material property input at the average temperature of each casing and frame, temperature dependent material property tables were included in the model so that at each element temperature, mechanical properties are evaluated for the element stiffness calculation in MSC/NASTRAN.

For the casing, frame and bearing housing assembly, corresponding to bolted joints, adjacent flanges were connected. The axial force distribution in all the flange joints were evaluated due to the internal pressure and temperature loading using MSC/NASTRAN. For any bolted joint flange assembly, if the joint is subjected to tensile load, heeling takes place at the outer diameter of the flange and if the joint is under compressive load, then heeling takes place at the inner diameter of the flange. Based on the axial force distribution in the flange joints, either outer diameter of the flanges are connected together if the joint is under tension or inner diameter of the flanges are connected together if the joint is under compression. This procedure helps in assembling the finite element models of all the casings, frames and bearing housings at the exterior grids for the superelement analysis(Fig.4). This satisfy the condition that adjacent elements interact only through common values of the boundary displacements[4].

BOUNDARY CONDITIONS

The complete engine structure is held by three point supports; two trunnion supports at the front in the inter casing region(3 and 9 o' clock positions), and one support at the rear in the exhaust-cone region(12 o' clock position). The three mounts are placed such that there are no expansion conflicts in the entire outer surface of the engine shell structure(Fig.4a). The front mounting point was chosen to allow zero axial displacement.

ASSUMPTIONS AND STRATEGY

Radial and axial displacements at three angular locations, namely, 12 o' clock, 3 o' clock and 6 o' clock positions were computed. It was assumed that the displacements were symmetric with respect to the chosen line of symmetry. To arrive at fairly circular shape for fan, compressor and turbine casings, various modifications such as geometry, stiffness alterations by changing shell thicknesses and the position of mounting blocks, improved temperature distribution and reorientation of the tie-rods between the load ring and the exhaust cone outer case and flange interface conditions were carried out. Typically, stiffness was altered by thickness change.

COLD LAY-UP

From the hot gas flow-path, i.e., hot dimensions of the engine structural assembly, deflections were computed for a typical flight condition with the superelement analysis of MSC/NASTRAN. The temperature and pressure distributions along the engine length are shown in Fig.5 and Fig.6 respectively. For the first iteration, cold dimensions were derived based on the differences in the axial and radial displacements obtained from the finite element model of the hot gas flow-path geometry. The cold dimensions were arrived at iteratively with circularity of the casings as one important consideration. These cold dimensions were improved upon till the hot gas flow-path dimensions are arrived at.

RESULTS AND DISCUSSIONS

From the radial displacement distribution it was observed that the casings especially those of fan, compressor and turbine modules become non-circular. However, the Von-Mises stress in all the casings and frames were very low, in some cases even below 20% of the 0.2% proof strength of the material. Since the non-uniform clearances at the rotor tips affect the performance and structural integrity of the compressor and turbine, it is essential that the fan, compressor and turbine casings are fairly circular when they are hot.

Radial displacements along the engine length for 12, 3 and 6 o' clock positions were plotted and it was found that there was a phase difference of 180 degrees between the 3 o' clock and 12(6) o' clock positions. This non-circularity was initially considered to be due to the low stiffness of the frames at the front and the rear. Though improved stiffness at the frames and also thick shell casings did not improve the circularity of the casings, balancing of axial force due to pressure distribution in the assembly was identified and studied in detail.

Sensitivity study of the axial force distribution on the casing circularity was carried out. Internal pressures acting at the inclined surfaces of the casings develop axial force either towards front or rear of the engine. Also axial forces are developed because of the pressure difference at either side of the rotor assembly, blade-disc stages, stator blades and the seals used to control the gas flow. The resultant of these axial forces are calculated and compared with the engine exhaust thrust. If the resultant force is not equal to the engine thrust, the inclination of the casing shell surfaces are altered such that the axial force equal to the engine thrust. This axial force balancing is one of the main tasks in the engine structural analysis. Before this balancing one can easily observe that the fan case become oval which distort the circularity of the casing leading to non uniform clearance between the casing inner surface and the rotor tip. The bearing housings which support the rotor assembly are connected to the inner diameter of the frames. Since the outer diameter of these frames are assembled with the flanges of non circular casing shells, the axis of the engine is distorted which further produce non uniform clearance at the rotor tip causing either rubbing or loss of the aerodynamic performance. Hence in the structural deflection analysis of an engine, axial force balancing is one of the important criteria to be considered.

This force balancing improved the circularity of the casings when they are hot as shown in Fig.7. The radial displacements of the casings are indicated from inlet case to exit of the augmentor liner, for 12, 6 and 3 o' clock positions, looking from rear of the engine. (In this plot, eight partitions were made to represent the axial positions of the inlet case, fan case, inter case, compressor case, combustor outer case, turbine case, exhaust cone and augmentor liner). There was still residual non-circularity at the inlet of the engine due to about 20% of the axial force that could not be balanced. From Fig.7, it was found that roundness of the casings was distorted throughout axial length of the engine structure. It is to be noted that the position of major axis of the ovality changes by 90 degree from middle of the third partition(inter case), due to the fact that axial freedom was constrained only at the inter case(3 and 9 o' clock positions).

In the initial design, the mounting blocks at 3 and 9 o'clock locations of the inter case were not bridging the front flange to the rear flange. From the analysis, large distortions were noticed in the inlet flange of the frame. The blocks were then extended from flange to flange(Fig.8), so as to increase the axial stiffness at the front mount. This modification showed a marked improvement in radial deflection at the flanges.

The exhaust frame and the load ring of the engine(Fig.2) are connected by means of 8 tie rods having spherical joints at either ends(Fig. 9). The end conditions are so chosen to arrest transmission of displacements (rotations and translations) from the inner structure to the outer and transmit only the radial bearing loads to the rear mount. The initial configuration selected induced severe distortion in radial deflection pattern and its effect could be felt up to the compressor casing. In the redesign cycle, the tie rods were oriented to have two perpendicular planes of symmetry (12-6, 3-9 clock locations). The reorientation of tie rods between the load ring and the exhaust cone outer case yielded significant result, by reducing circular distortion(from fourth partition to seventh partition in Fig.7).

From the strain energy distribution (Fig. 10) of the engine structure(Fig. 2), the shell thickness of the candidate casings/frames was optimized, taking into account the availability of the forged sheets, casting and machinable wall thicknesses. A FORTRAN code was developed to apply the thickness constraints to the candidate cases/frames by altering the shell thicknesses. With a few set of iterations, a weight reduction of about 22 percent was achieved by marginally increasing the strain energy levels in the shells and flanges, keeping the stress levels below the allowable stress limits.

With the above experience for the weight reduction and the need to have fairly circular casings when it is hot, a new scheme for the engine structure was considered as shown in Fig. 11. The deflection pattern for the new scheme is shown in Fig.12 for which the axial force is fully balanced(Fig. 13). The addition of the inlet frame improved the circularity of the fan case. Also, the additional/improved frames in the new configuration were considered to take into account the shaft critical speeds to be away from the idling to maximum RPM range. In the low temperature area Titanium alloys were considered for the bearing housings and frames as compared to Nickel alloy of the earlier engine configuration 1. Though the former is a light alloy with low Young's modulus, the geometry was optimized for the stiffness as in the earlier configuration.

CONCLUSIONS

Super element analysis of MSC/NASTRAN to obtain the cold lay-up from the hot gas flow-path for a typical aero engine structural assembly is given. The effect of modified stiffness distribution due to (a) addition of front frame and (b) modifications to improve the existing frames is demonstrated by improved circularity of the casings when the engine is hot(Fig.12). It should be noted that this is made possible only after taking into account the axial force balance and altering the strain energy distribution in the total structure for the engine weight optimizatioin.

ACKNOWLEDGMENTS

The authors express their gratitude to the Director, Gas Turbine Research Establishment, Bangalore, India for permitting to submit the above work for the 1997 MSC Aerospace User's Conference to be held in Los Angeles, California, USA.

REFERENCES

1. Bellamy, R.A., Bennett, I.C. and Elston, S.T., 'Development of a correlated finite element dynamic model of a complete aero engine'. ASME 81-DET-74.

2. Bedrossien, H. and Phoenix, R., 'Application of structural optimization technique to reduce the external vibrations of a gas turbine engine'. ASME 81-DET-143.

3. R.R. Craig, and M.C.C Bampton, 'Coupling of substructures for Dynamic Analysis', AIAA Journal, Vol. 6, No.7, July 1968.

4. MacNeal, R.H., 'Finite Elements: Their Design and Performance', 1994.

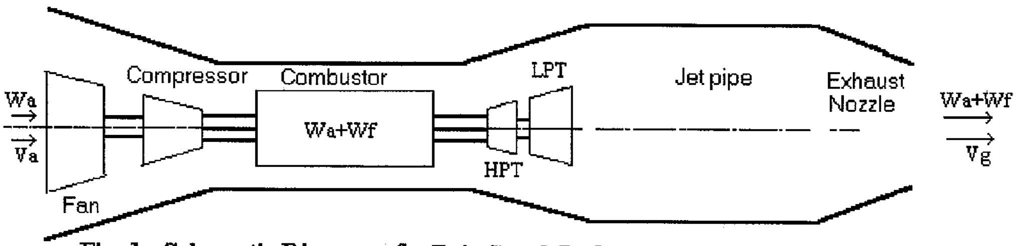

Fig.-1 : Schematic Diagram of a Twin Spool Jet Engine

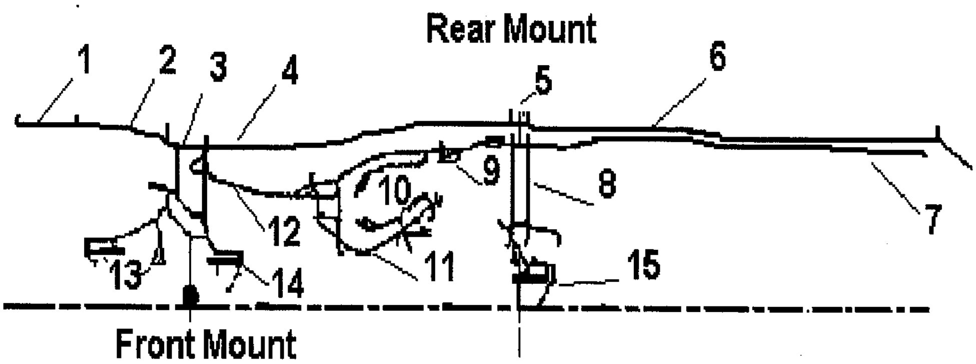

Fig. 2 Engine Configuration 1

1 INLET CASE
2 FAN CASE
3 INTER CASE
4 FAN DUCT
5 LOAD RING
6 AUGMENTOR DUCT
7 AUGMENTOR LINER
8 EXHAUST CONE
9 TURBINE CASE
10 COMBUSTOR LINER
11 COMBUSTOR CASE
12 COMPRESSOR CASE
13 BEARING HOUSING #1 & #2
14 BEARING HOUSING #3
15 BEARING HOUSING #5

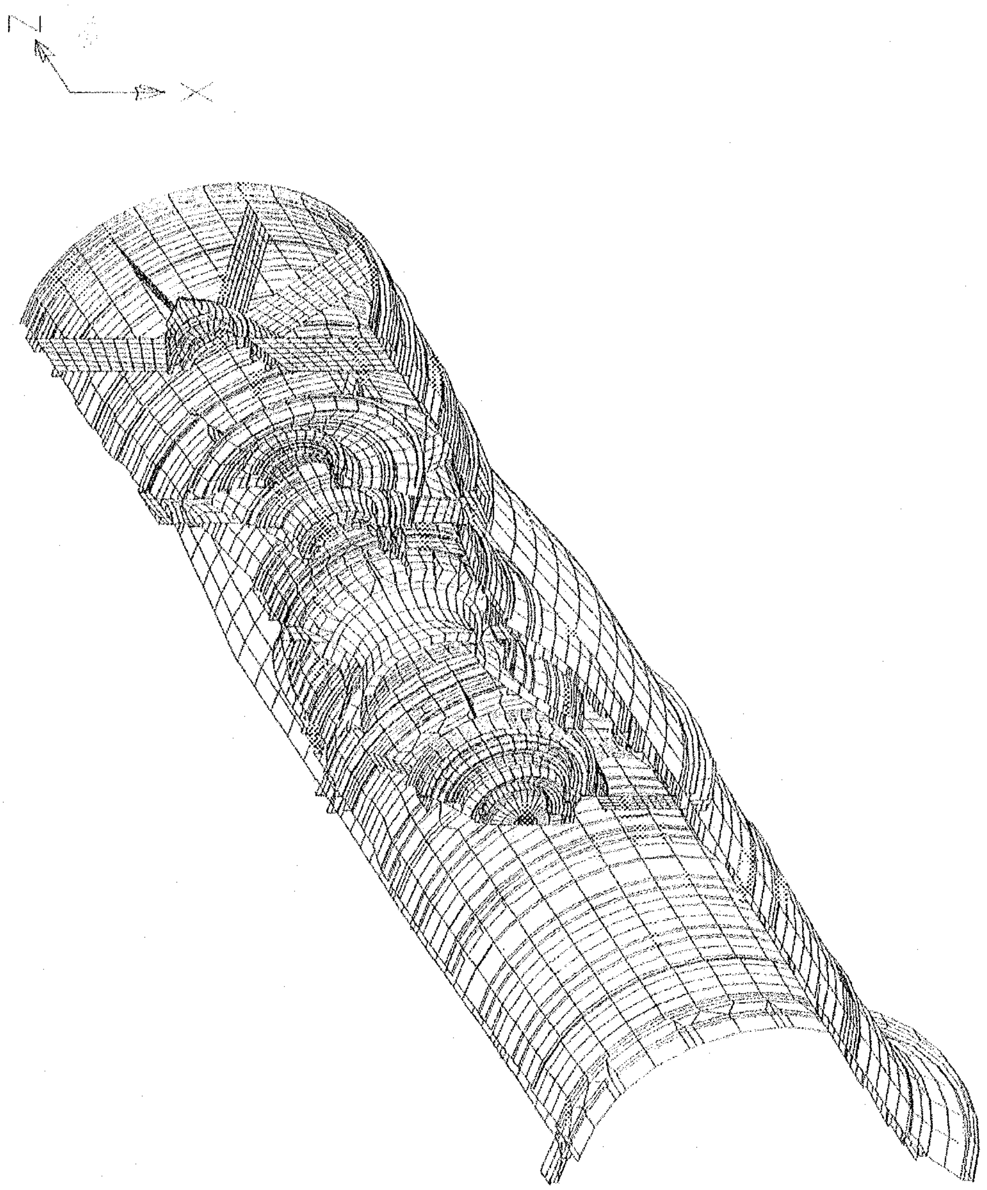

Fig. 3 Finite Element Model of Engine Structure
(Grids=12000, Elements=13000, DOF=60000)

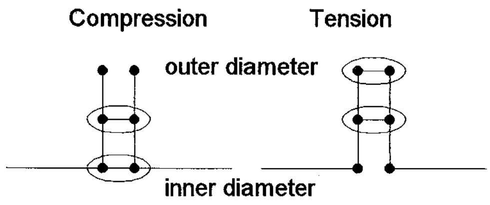

Fig. 4 Flange Joint

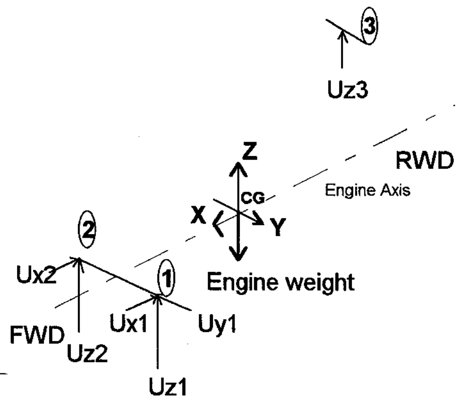

Fig.4a Degrees of Freedom(Ux,Uy,Uz) for Engine mounts(1,2,3)

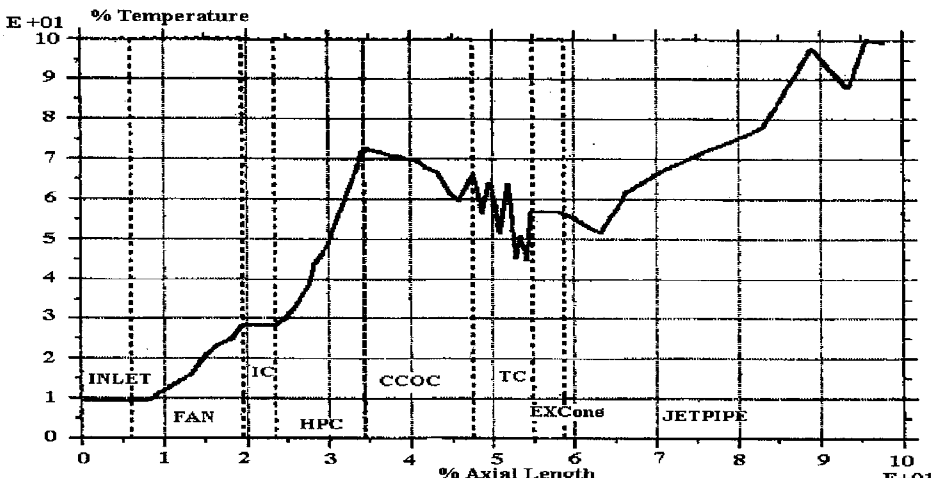

Fig.-5 : Temperature Distribution (Core)

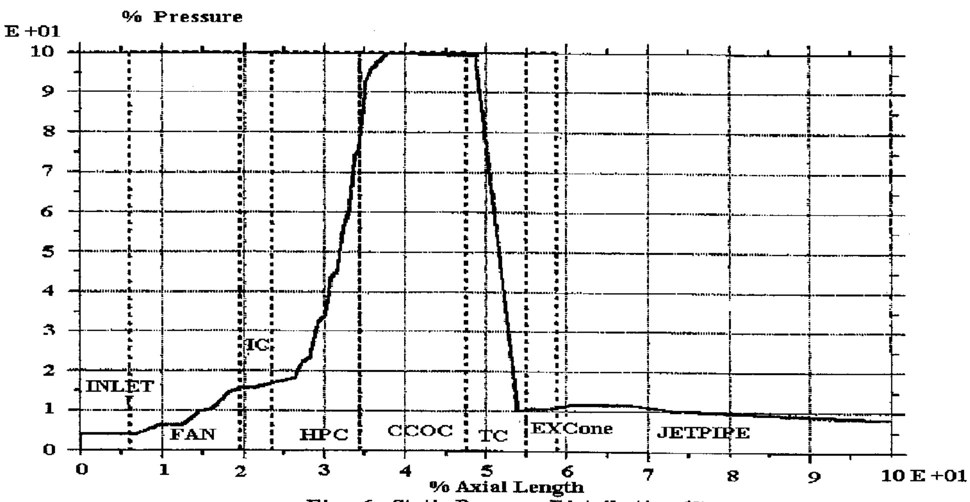

Fig.- 6 : Static Pressure Distribution (Core)

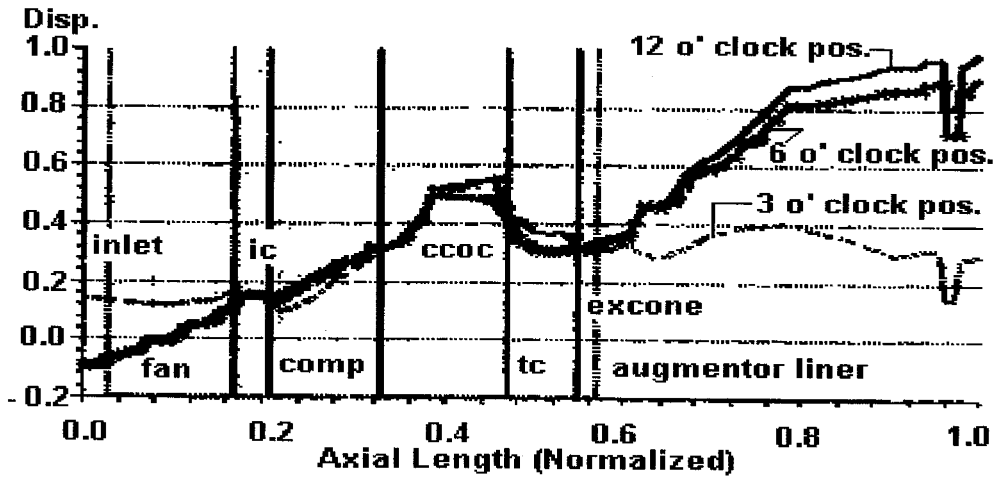

Fig. 7 Normalized radial Disp. for Engine Config. 1

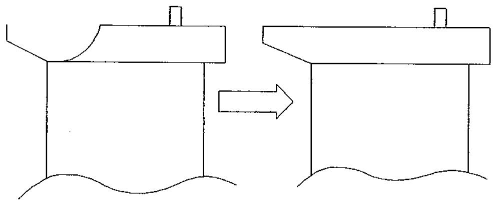

Fig. 8 Front Mount Block

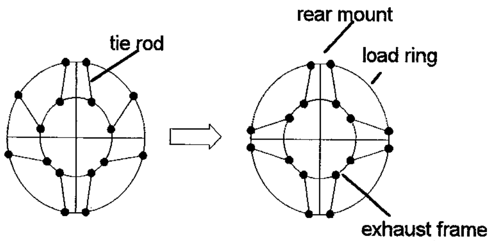

Fig. 9 Tie Rod Orientation

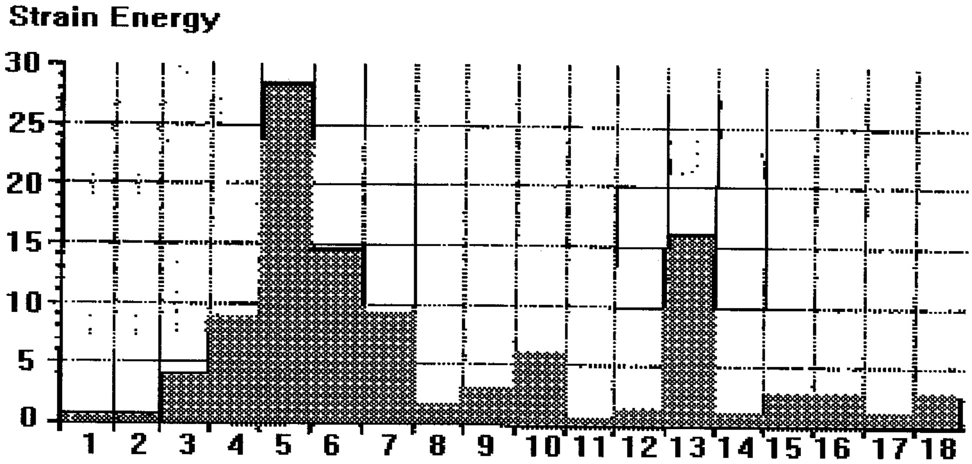

Fig. 10 Percentage Strain Energy for Engine Config. 1

1 INLET CASE
2 FAN CASE
3 INTER CASE
4 COMPRESSOR CASE
5 COMBUSTOR CASE
6 COMBUSTOR LINER
7 TURBINE CASE
8 LP SHROUD RING
9 HP SHROUD RING
10 EXHAUST CASE
11 LOAD RING
12 AUGMENTOR DUCT
13 AUGMENTOR LINER
14 FAN DUCT
15 BEARING HOUSING #1
16 BEARING HOUSING #2
17 BEARING HOUSING #3
18 BEARING HOUSING #5

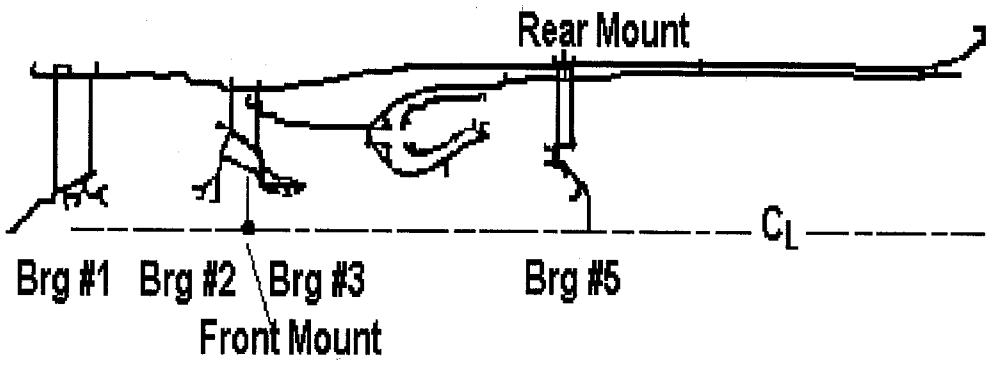

Fig. 11 Modified Engine Configuration

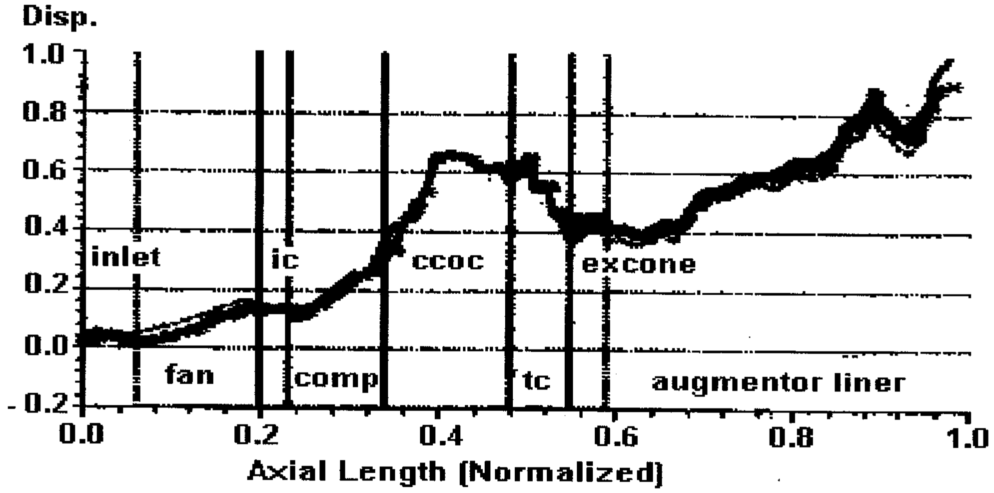

Fig. 12 Normalized Radial Disp. for Engine Config. 2

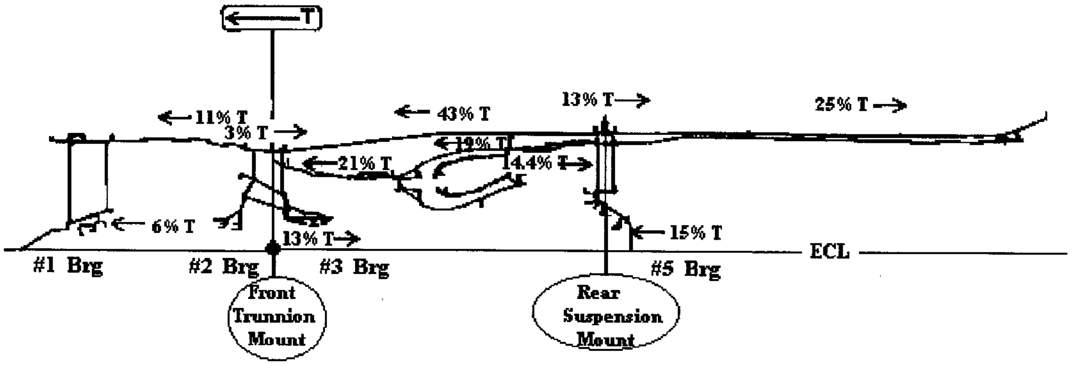

Fig. 13 Percentage Axial Force distribution in Engine Config. 2